HAL
open science

Detection and Characterization of Precipitates in Annealed Cz Silicon Wafers

Caroline Veve, Nathalie Gay, Michäel Stemmer, Santo Martinuzzi

To cite this version:

Caroline Veve, Nathalie Gay, Michäel Stemmer, Santo Martinuzzi. Detection and Characterization of Precipitates in Annealed Cz Silicon Wafers. Journal de Physique III, 1995, 5 (9), pp.1353-1363. 10.1051/jp3:1995195 . jpa-00249385

HAL Id: jpa-00249385

https://hal.science/jpa-00249385

Submitted on 4 Feb 2008

HAL is a multi-disciplinary open access archive for the deposit and dissemination of scientific research documents, whether they are published or not. The documents may come from teaching and research institutions in France or abroad, or from public or private research centers.

L'archive ouverte pluridisciplinaire **HAL**, est destinée au dépôt et à la diffusion de documents scientifiques de niveau recherche, publiés ou non, émanant des établissements d'enseignement et de recherche français ou étrangers, des laboratoires publics ou privés.

J. Phys. III France 5 (1995) 1353–1363

Classification
Physics Abstracts
61.70 — 72.10

Detection and Characterization of Precipitates in Annealed Cz Silicon Wafers

Caroline Veve, Nathalie Gay, Michäel Stemmer and Santo Martinuzzi

Laboratoire de Photoélectricité des Semi-Conducteurs E.A. 882 "Défauts dans les Semiconducteurs et leurs Oxydes", Faculté des sciences et techniques de Marseille-St. Jérôme, 13397 Marseille Cedex 20, France

(Received 19 December 1994, revised 2 May 1995, accepted 24 May 1995)

Abstract. — A Scanning InfraRed Microscope (S.I.R.M.), a Light Beam Induced Current mapping (L.B.I.C.), a Fourier Transform infrared spectroscope (F.T.I.R.), and a minority carrier diffusion length measurements tool have been associated to detect precipitates in annealed Czochralski (Cz) silicon wafers and to evaluate their recombination strength with or without metallic contamination. The influence of a phosphorus diffusion was also investigated. After two step annealings (750 °C - 16 h and 900 °C - 24 h or 96 h) S.I.R.M. reveals the presence of precipitates, while L.B.I.C. maps display a ring-like distribution of recombination centers and minority carrier diffusion length (L_n) collapses to 2 μm. Copper contamination does not significantly modify the preceding observations when precipitates are formed. Phosphorus diffusion near the surface shrink the precipitates revealed by M.I.R.B. but do not suppress the ring-like patterns in the L.B.I.C. maps and L_n increases slightly. These results suggest that the recombination strength of precipitates does not depend on a metallic decoration but more probably on interfacial states between the precipitates and the host crystal or on associated extended defects.

1. Introduction

Czochralski-grown (Cz) silicon wafers used for electronic and microelectronic devices contain a large concentration of oxygen atoms. Generally, these atoms are dissolved as interstitials, and the solution is supersaturated at low temperature. The concentrations are close to 10^{18} cm^{-3} and during wafer processing precipitates are easily formed.

Although dissolved oxygen is electrically neutral, oxygen precipitates (O_p) degrade p-n junctions used to isolate integrated transistors, and both the recombination as well as the generation lifetime [1].

These precipitates have been largely studied because they are used for internal gettering of metallic impurities. Their nucleation, growth, morphology, and chemical composition are known and almost completely understood [2, 3]. Several macroscopic and microscopic techniques have been used to get these informations and they were more recently completed by detection techniques which are able to localize the position of precipitates and to evaluate

© Les Editions de Physique 1995

their density like the infrared laser tomography [4, 5]. However the nature of the recombination centers which causes the lifetime degradation when O_p are formed was not established clearly. These centers could be due to surface states associated to extended defects, or to trapped metallic impurities [1, 6, 7]. In addition, their reaction with point defects, especially with interstitial silicon atoms is also not well known.

The present paper attempts to give additional informations about these problems by the use of suitable experimental techniques able to detect the presence of precipitates and to evaluate their recombination strength. Particularly non destructive techniques were used like: Scanning InfraRed Microscopy (S.I.R.M.), Light Beam Induced Current (L.B.I.C.) mappings, associated with Fourier Transform InfraRed spectroscopy (F.T.I.R.).

2. Experimental

P-type Cz silicon wafers (boron doped: 10^{15} cm^{-3}) both sides polished, containing about 10^{18} cm^{-3} interstitial oxygen atoms were annealed in pure argon at 750 °C for 16 h and then at 900 °C for 24 h or 96 h, in order to create nucleation sites and growth the precipitates respectively. Some samples were also submitted to diffusion of copper at 950 °C for 1 h in argon flow (the copper was deposited on one face of the sample by electron-gun evaporation). Annealed and copper-diffused samples were also submitted to a phosphorus diffusion from a $POCl_3$ source at 900 °C for 4h, in order to inject an excess of self interstitials (Si_i) in the material.

Table I summarizes the nature and the purpose of the different treatments applied to the investigated samples.

Interstitial oxygen concentration [O_i] was determined at room temperature by F.T.I.R. spectroscopy using the conversion coefficient 3.03×10^{17} cm^{-3} [8].

Minority carriers diffusion lengths L_n were determined from the spectral variations of the photocurrent and of the light absorption coefficient in the near infrared ($860 < \lambda < 980$ nm). The current collecting structures were semitransparent Al-Si diodes or *p-n* junctions.

The L.B.I.C. system, designed to get photocurrent and diffusion length maps has been already described [9] and we recall only that the light spot diameter was below 10 μm when the wavelengths varied between 800 and 1000 nm.

A schematic block-diagram of the S.I.R.M. system, designed according to earlier suggestions by Booker *et al.* [10] is reported in Figure 1. A monochromatic beam from a semiconductor laser diode ($\lambda = 1300$ nm) is focused on and in the sample. The transmitted beam is detected by a germanium diode. The laser diode is modulated by a function generator and a lock in amplifier is used to reduce the noise. Attenuation of the transmitted beam occurs at the interface of precipitates and of the silicon host crystal due to the light reflection at the border of two phases of different dielectric constant. Thanks to the concentration of the light intensity by the focalisation, the attenuation is high if a precipitate is found just in the focus volume, and low or zero if it is out of the focus point. By scanning in the x, y, z directions every point in the sample can be assessed and probed for the presence of precipitates. A three-dimentional picture of the sample can be obtained and precipitates can be detected even with a size as small as 0.1 μm. The resolution is about 2-3 μm. The contrast obtained when the precipitate is metallic in nature is higher compared to that given by a dielectric one. This is a consequence of the Mie's theory as developped in reference [11].

Sirtl and Secco etching solutions have been used to reveal the presence of precipitates in the ring like patterns.

Float-zone (FZ) samples, used as reference, were submitted to the annealing treatments (a) and (a+b) of Table I.

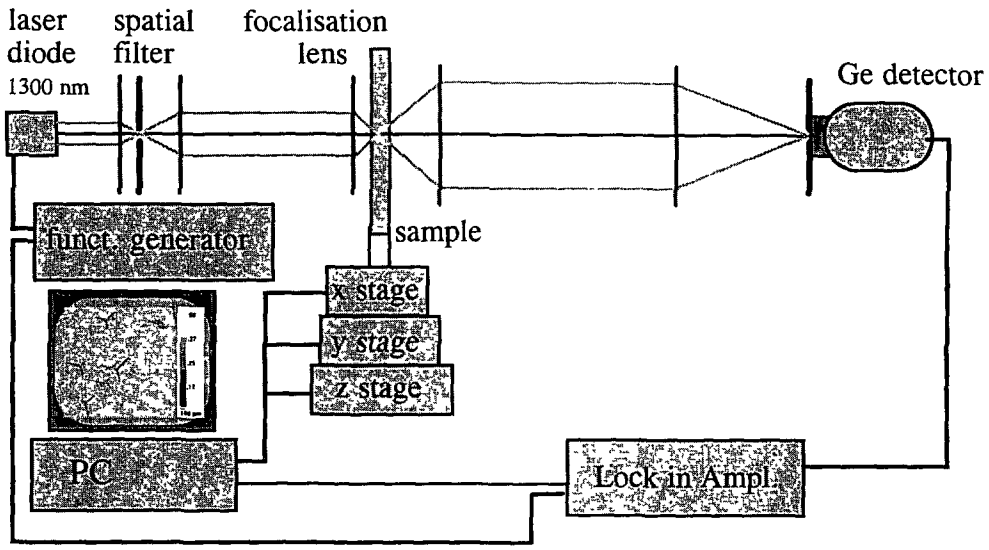

Fig. 1. — S.I.R.M. set-up.

Table I. — *Nature and purpose of the different treatments applied to the investigated samples (All treatments, except c, were carried out under an Argon flow).*

Label	Treatment	
	Nature	**Goal**
(a)	Preannealing : 750°C-16h	Nucleation
(b1)	(a) + Annealing : 900°C-24h	Growth
(b2)	(a) + Annealing : 900°C-96h	Growth
(c)	Phosphorus diffusion : 900°C-4h (from $POCl_3$)	Si_i injection
(d)	Copper diffusion : 950°C-1h	Contamination
(e)	Annealing : 900°C-4h	Blank for (c)
(f)	Annealing : 950°C-1h	Blank for (d)

3. Results

Table II displays the results obtained before and after the different annealing treatments.

In the as-received samples the values of L_n are higher than 200 μm and homogeneously distributed all over the wafer (as verified by the L.B.I.C. maps). No precipitates are revealed by S.I.R.M. and by F.T.I.R..

Preannealed samples (treatment (a)) are characterized by a degradation of L_n, which collapses to 15 μm, by the absence of precipitates revealed by S.I.R.M., and also, by a ring-like dis-

Table II. — *S.I.R.M., F.T.I.R. and L.B.I.C. results obtained before and after the different annealing treatments applied to the investigated samples (O_p = oxygen precipitates).*

Material treatment	As-grown	Preannealed (a)	Annealed (a)+(b1)	Annealed (a)+(b2)	Annealed & gettered (a)+(b1)+(c)
F.T.I.R. main absorption band(s) (cm^{-1})	1107 --> $[O_i]$ #10^{18}	1090 --> O_p	1080 & 1225 --> O_p	1080 & 1225 --> O_p	1120 & 1225 --> O_p
S.I.R.M.	no precipitates	no precipitates	precipitates (different size & contrast)	precipitates (different size & contrast)	no precipitates
Diffusion length L.B.I.C.	L # 200 µm homogeneous	L # 15 µm ring-like	L # 2 µm ring-like	L # 2µm ring-like	L # 7 µm ring-like

tribution of photocurrent in L.B.I.C. maps. Simultaneously, an absorption band at 1090 cm^{-1} appears in the IR spectrum, which could be due to the formation of nucleation centers.

In two-step annealed samples (treatment (a+b)) the S.I.R.M. detects the presence of precipitates, the density of which is, for a treatment at 900 °C, larger after 24 h than after 96 h, as shown in Figures 2 and 3. The L.B.I.C. map reveals a ring-like distribution of recombination centers (Fig. 4) while L_n decreases to 2 μm. Two absorption bands located at 1080 and 1225 cm^{-1} appear in F.T.I.R. spectroscopy. The band at 1080 cm^{-1} is attributed to SiO_x amorphous precipitates, and that at 1225 cm^{-1} is characteristic of platelet precipitates [12,13].

When the same treatment ((a+b)) is applied to FZ samples, no precipitates are detected, indicating that there is no contamination of the wafers during the annealing steps, and that the observed precipitates are related to the impurities contained in the Cz wafers, so certainly to oxygen atoms.

In the two-step annealed and phosphorus diffused samples (treatment (a+b+c)), no precipitates can be revealed by S.I.R.M. The absorption band at 1080 cm^{-1} has disappeared and is replaced by another one at 1120 cm^{-1}, while that at 1225 cm^{-1} is always present, as the ring like distribution in the L.B.I.C. map. The mean value of L_n increases to 7 μm.

Note that the ring like structure observed by L.B.I.C. maps is also revealed by chemical etchings, as shown in Figure 5.

The thermal treatment of the phosphorus diffusion, i.e., treatment (e) (900 °C for 4 h in argon) has also been applied to as-grown and two-step annealed samples, in order to separate the effect of P-diffusion from that of annealing. In as-grown samples, this treatment leads to decrease $[O_i]$ to about 5×10^{17} cm^{-3}, to the formation of precipitates visible by S.I.R.M. and to the appearence of the ring like distribution in L.B.I.C. maps, while L_n decreases to about 40 μm. In the two-step annealed samples with the longer growth time (treatment (a+b2)), there is an increase of the size and density of precipitates in S.I.R.M. images, while in the other two-step annealed samples (a+b1) there is not any marked change in the S.I.R.M. images, after the additional treatment.

These results suggest that a redissolution of the oxygen precipitates occurs during the long treatment, especially those that have not reached a critical size [14].

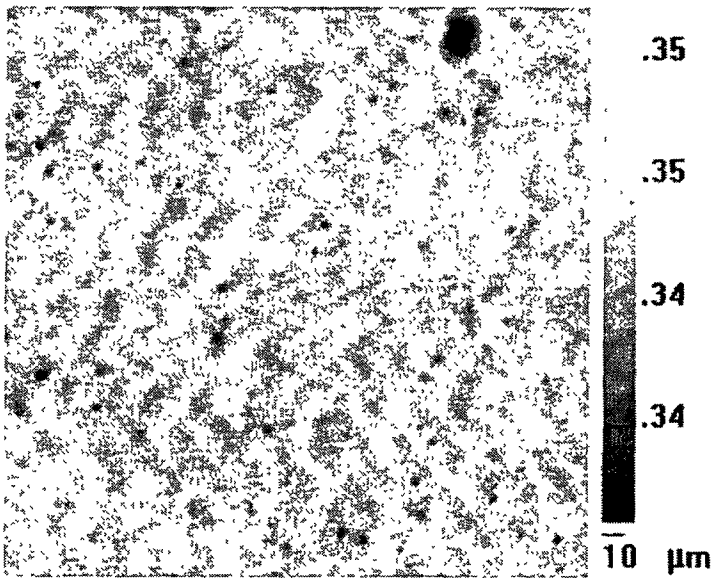

Fig. 2. — S.I.R.M. image of a sample after the treatments (a) and (b1) (the relative grey level scale corresponds to different rates of transmitted light).

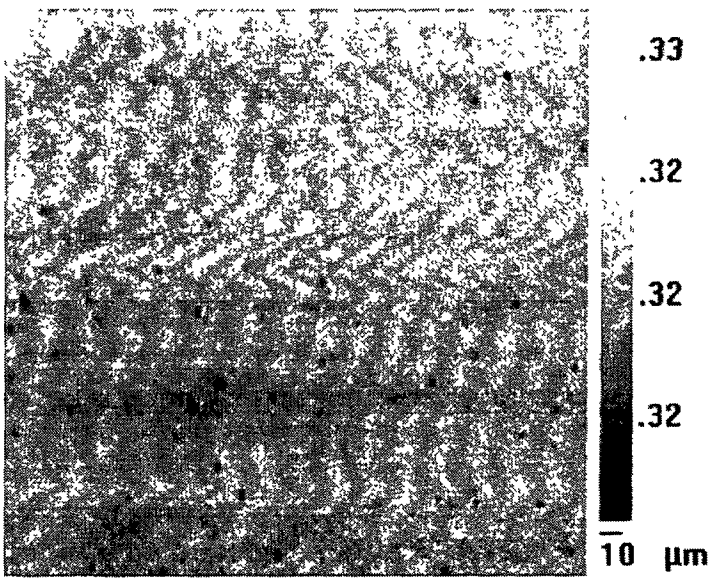

Fig. 3. — S.I.R.M. image of a sample after the treatments (a) and (b2) (the relative grey level scale corresponds to different rates of transmitted light).

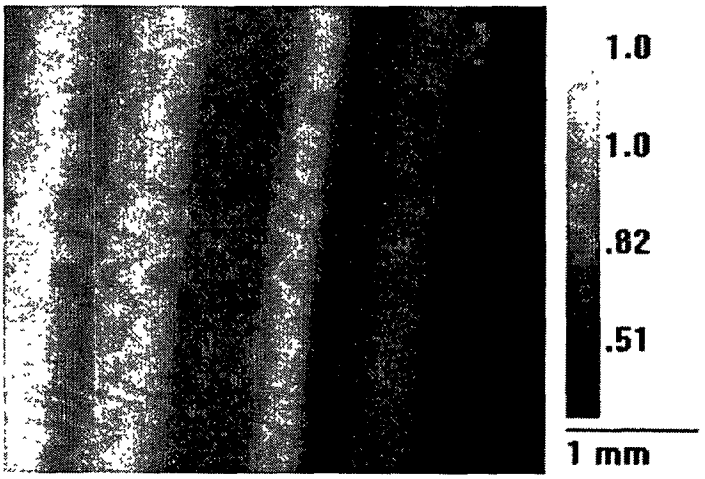

Fig. 4. — L.B.I.C. photocurrent map of a sample after the treatments (a) and (b).

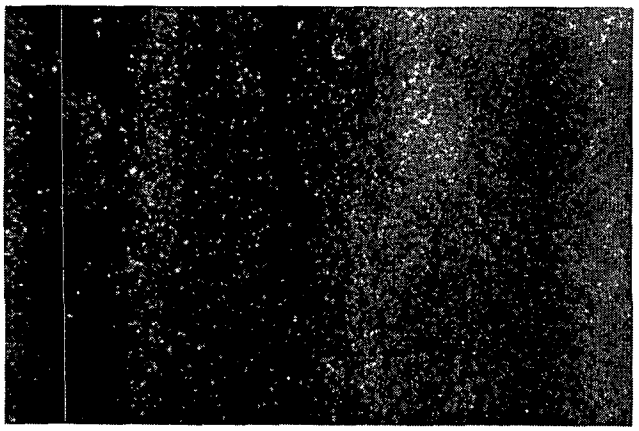

Fig. 5. — Microphotography (optical microscope, dark field) of the two-step annealed samples after Sirtl etch, showing the ring-like distribution of the precipitates.

Results concerning the influence of a copper diffusion are given in the Table III. The introduction of copper in the as-received samples (treatment (d)) gives new features of precipitates. As shown in Figure 6 star-shaped colonies of precipitates are visible in the S.I.R.M. images, as already observed by Laczik *et al.* [15]. This well-known particular precipitation is due to the high rate of silicon self interstitial emission when the $SiCu_3$ phases are formed during the "slow" cooling down. The S.I.R.M. indicates also that the density of the star-shaped precipitates is higher near the free surfaces of the wafers than in the bulk. This is due to the absorption by these surfaces of the self interstitials emitted during the formation of copper precipitates. The oxygen concentration does not vary.

In the contaminated and two-step annealed samples (treatment (a+b+*d*)), oxygen- and

Table III. — *S.I.R.M., F.T.I.R. and L.B.I.C. results obtained before and after the different annealings and Cu contamination treatments applied to the investigated samples (O_p & Cu_p = oxygen and copper precipitates).*

Material treatment	As-grown & Cu contaminated (d)	Annealed & Cu contaminated (a)+(b1)+(d)	Annealed & Cu contaminated & gettered (a)+(b1)+(d)+(c)
F.T.I.R. main absorption band(s) (cm^{-1})	1107 --> $[O_i]\#10^{18}$	1080 & 1225 --> O_p	1120&1225 --> O_p
S.I.R.M.	typical colonies of Cu precipitates	precipitates corresponding to O_p & Cu_p	no precipitates
Diffusion length L.B.I.C.	homogeneous	L # 2μm ring-like	L # 7μm

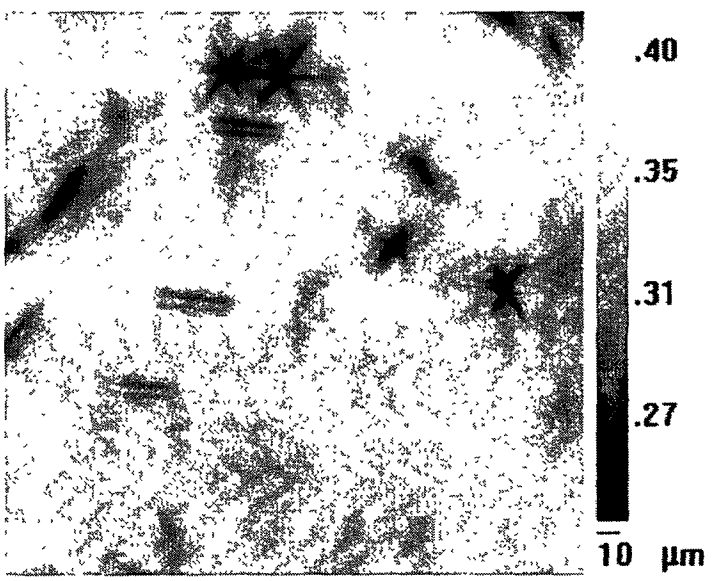

Fig. 6. — Star-shaped colonies of Cu precipitates observed by S.I.R.M. after treatment (d).

copper-related precipitates are revealed by S.I.R.M., as shown in Figure 7. The comparison of Figures 6 and 7 suggests that, when oxygen precipitates are present, copper atoms precipitate around them: the size of the metallic precipitates in Figure 7 is smaller than in Figure 6, since copper is precipitated on a larger quantity of nucleation sites. The L.B.I.C. maps and the measure of L_n give results similar to those obtain with the two-step annealed and non-

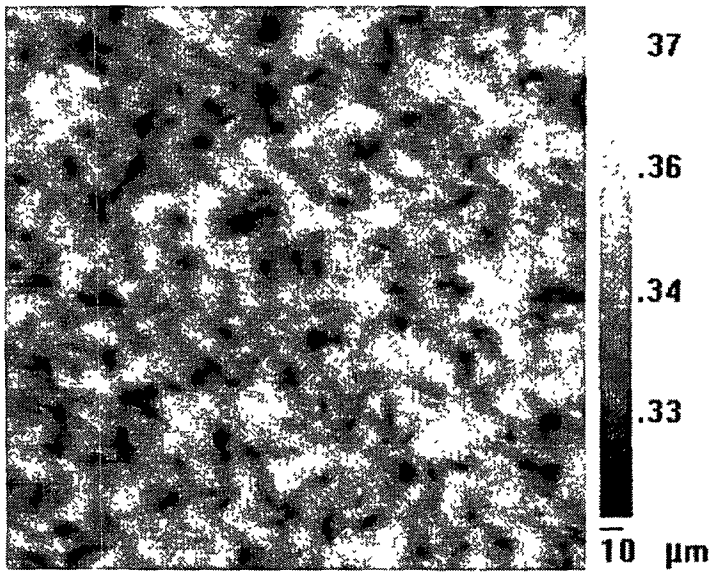

Fig. 7. — S.I.R.M. image of a two-step annealed and Cu-contaminated sample.

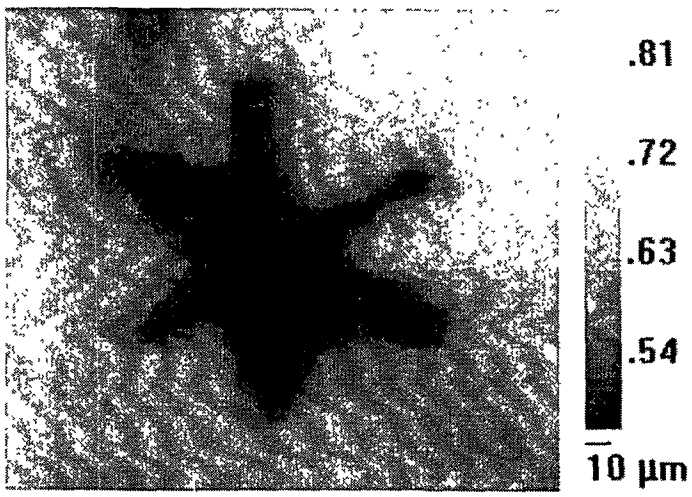

Fig. 8. — L.B.I.C. photocurrent map of a star-shaped colony of Cu precipitates observed after treatment (d).

contaminated samples: ring-like distribution and L_n # 2 μm. In addition, in the L.B.I.C. maps, the star-shaped forms appear as regions of very poor photocurrent intensity, which are well correlated with the position of copper precipitates as shown in Figure 8.

The harmlessness of copper is also verified by the contamination of as-received wafers: the value of L_n is the same after a thermal treatment at 950 °C for 1h with or without copper

contamination (treatment (d) or (f), respectively). $[O_i]$ is also not modified.

The diffusion of phosphorus (treatments (a+b+d+c)) leads to the disappearence of copper precipitates in non-annealed, as well as in annealed, samples.

The comparison of Tables II and III suggests that the copper contamination does not modify the results obtained after the two-step annealings and also those observed after the two-step annealings followed by a phosphorus diffusion

4. Discussion

The S.I.R.M. used in this work is able to reveal oxygen-related and metallic precipitates in silicon, provided they have a sufficient size (at least 0.1 μm). After two-step annealings, F.T.I.R. spectroscopy indicates that the images observed by S.I.R.M. are due to the formation of SiO_x amorphous precipitates (1080 cm^{-1}). These precipitates have a high recombination strength, because when they are present, L_n decreases to 2 μm.

The ring-like structure, revealed by L.B.I.C. after annealing of the samples, is generally attributed to oxygen striations and to Oxydation Stacking Faults (O.S.F.). In the present work this structure is associated with an absorption band at 1225 cm^{-1} corresponding to platelet precipitates. These results could be explained by the presence of oxygen striations in the as-grown wafers, and by the emission of self interstitial atoms when the amorphous precipitates are formed. These self interstitials contribute to the formation of O.S.F. and of platelet precipitates, which follow the oxygen striations. These crystallographic defects and precipitates have also a recombination activity because they limit L_n to 7 μm, after the phosphorus diffusion which schrinks the precipitates observed by S.I.R.M.. This shrinkage of the precipitates is certainly due to the injection of self interstitials in the bulk of the samples during the phosphorus diffusion. It was explained by the interaction of self interstitials with precipitates which contain fewer silicon atoms per unit volume than the silicon lattice [16,17].

The recombination strength of the precipitates is not related to the trapping of impurities; their decoration by copper, like the removal of these atoms has no effect on L_n and on the ring-like L.B.I.C. patterns. In terms of recombination strength of minority carriers, there is no interaction between the precipitates, the extended defects and copper atoms. It could be reasonable to ascribe recombination centers to intrinsic surface states of amorphous SiO_x precipitates, and to the extended defects involved in the ring-like patterns.

As shown by Figure 4, there is a poor contrast between the different patterns in the L.B.I.C. maps, indicating that other recombination centers are homogeneously spreaded in the entire wafer. They are not detected by S.I.R.M. or by L.B.I.C., probably due to their small size. Like the concentration of self interstitials is very large due to their emission during the precipitation or during the phosphorous diffusion from $POCl_3$, it could be assumed, with Schmalz *et al.* [6] that clusters of Si_i are formed, associated with small O_{ps}. Such clusters cannot be removed or shrunk during phosphorous diffusion and that explains why the values of L_n remain low after this gettering treatment (i.e., 7 μm).

The disagrement between the S.I.R.M. and the L.B.I.C. images of the material, i.e., the amorphous SiO_x precipitates are revealed by S.I.R.M. but do not appear in the L.B.I.C. maps, could be explained by the lack of resolution of the last technique in a degraded material. Indeed L.B.I.C. scan lines and maps are sensitive to the presence of recombination centers when the diffusion length of minority carriers is larger than the spot size (# 10 μm). If L_n is too small, as it is the case in the two step annealed samples, the contrast is insufficient and the L.B.I.C. maps reveal only the ring like distribution because the size of the patterns is larger than that of the spot.

5. Conclusion

S.I.R.M. and L.B.I.C. are two non destructive techniques which are able to reveal the presence of neutral or (and) of electrically active precipitates in silicon. They can be associated to F.T.I.R. spectroscopy to get further information on precipitates types.

After two step annealing of oxygen rich samples, the S.I.R.M. reveal amorphous SiO_x precipitates, and L.B.I.C. maps shows the formation of ring like patterns containing probably platelet precipitates associated to extended crystallographic defects.

Contamination by copper at 950 °C followed by a slow cooling down has no effect on the mean value of the diffusion length of minority carriers, even when star-shaped precipitates are formed.

Injection of self interstitials by P-diffusion shrinks the amorphous SiO_x and the copper precipitates, while the ring like patterns are not modified.

The results suggest that the recombination strength of amorphous precipitates could result from interfacial states between SiO_x and Si matrix, while that of ring-like distributed precipitates is more related to associated extended defects. However cluster of self interstitials associated to small O_{ps} could participate to the recombination in the oxygen rich annealed samples.

Acknowledgments

This work was sponsored by CNRS-ECOTECH France, by ADEME France and by the European Union DG XII - JOULE II programme - Multichess II contract.

References

[1] Hwang J.M. and Schröder D., Recombination properties of oxygen-precipitated silicon, *J. Appl. Phys.* **59** (1986) 2476-2487.

[2] Endrös A.L., Properties of hydrogen, oxygen and carbon in Si, *Solid State Phenom.* **32,33** (1993) 143-154.

[3] Bender H. and Vanhellemont J., Oxygen related lattice defects in silicon: present status, *Mat. Res. Soc. Symp. Proc.* **262** (1992) 15-29.

[4] Fillard J.P., Gall P., Castagne M. and Bonnafe J., Laser scanning tomography: a study of the defec cluster nucleation and growth in silicon, *Solid State Phenom.* **6,7** (1989) 403-408.

[5] Moriya K. and Ogawa T., Observation of lattice defects in GaAs and heat treated Si crystal by infrared LST, *J. Appl. Phys.* **22** (1983) 207-210.

[6] Schmalz K., Kirscht F.G., Klose H., Richter H. and Tittelbach-Helmreich K., DLTS study on deep level defect in Cz-p-Si due to heat treatment at 600 to 900 °C., *Phys. Stat. Sol. (a)* **100** (1987) 567-582.

[7] Vanhellemont J., Simoen E., Bosman G., Claeys C., Kaniava A., Gaubas E., Blondeel A. and Clauws P., "On the electrical activity of oxygen-related extended defects in silicon", Semi Conductor Silicon, H.R. Huff, W. Bergholz and K. Sumino Eds. (Pennington, The Electrochem. Soc. 1994) pp. 670-683.

[8] Yatsurugi Y., Akiyama N., Endo Y. and Nozaki T., *J. Electrochem. Soc.* **120** (1973) 976-81.

[9] Stemmer M., Mapping of the local minority carrier diffusion length in silicon wafers, *Appl. Surf. Sci.* **63** (1993) 213-216.

[10] Booker G.R., Laczik Z. and Kidd P., The Scanning Infrared Microscope (SIRM) and its application to bulk GaAs and Si: a review, *Semicond. Sci. Technol.* **7** (1992) A110-A121.

[11] Stemmer M., Ph.D. Thesis, "Réalisation d'instruments automatisés de révélation et de caractérisation locale de défauts dans du silicium", University of Marseilles (Sept. 1994).

[12] Tempelhoff K., Spiegelberg F., Gleichmann R. and Wruck D., Precipitation of oxygen in dislocation free silicon, *Phys. Stat. Sol. (a)* **56** 213 (1979) 214-223.

[13] Sun Q., Yao K.H., Gatos H.C. and Lagowski J., Effect of nitrogen on oxygen precipitation in silicon, *J. Appl. Phys.* **71** (1992) 3760-65.

[14] Hu S.M., Oxygen precipitation in silicon, *Mat. Res. Soc. Symp. Proc.* **59** (1986) 249-267.

[15] Laczik Z., Booker G.R. and Falster R., Scanning infrared microscope investigation of oxide particle in Cz silicon heat treated for intrinsic gettering, *Solid State Phenom.* **6,7** (1989) 395-402.

[16] Kang J.J. and Schröder D.K., Gettering in silicon, *J. Appl. Phys.* **65** (1989) 2974-2985.

[17] Claeys C. and Vanhellemont J., Defects in crystalline silicon, Advanced and Semiconducting Silicon-Alloy Based Material and Devices, J.F.A. Nijs, Ed. (Inst. of Phys. Pub., Bristol, 1994) pp. 35-102.